

Tunability of the spin reorientation transitions with pressure in NdCo_5

Cite as: Appl. Phys. Lett. **116**, 102408 (2020); <https://doi.org/10.1063/1.5135640>

Submitted: 07 November 2019 . Accepted: 02 March 2020 . Published Online: 13 March 2020

 Santosh Kumar,  Christopher E. Patrick,  Rachel S. Edwards,  Geetha Balakrishnan,  Martin R. Lees, and  Julie B. Staunton



View Online



Export Citation



CrossMark

ARTICLES YOU MAY BE INTERESTED IN

[Observing relaxation in device quality InGaN templates by TEM techniques](#)

Applied Physics Letters **116**, 102104 (2020); <https://doi.org/10.1063/1.5139269>

[Thickness-dependent electron momentum relaxation times in iron films](#)

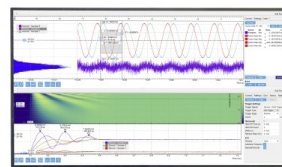
Applied Physics Letters **116**, 102406 (2020); <https://doi.org/10.1063/1.5142479>

[Easy-cone magnetic structure in \$\(\text{Cr}_{0.9}\text{B}_{0.1}\)\text{Te}\$](#)

Applied Physics Letters **116**, 102404 (2020); <https://doi.org/10.1063/5.0002118>

Challenge us.

What are your needs for periodic signal detection?



Zurich
Instruments



Tunability of the spin reorientation transitions with pressure in NdCo₅

Cite as: Appl. Phys. Lett. **116**, 102408 (2020); doi: [10.1063/1.5135640](https://doi.org/10.1063/1.5135640)

Submitted: 7 November 2019 · Accepted: 2 March 2020 ·

Published Online: 13 March 2020



View Online



Export Citation



CrossMark

Santosh Kumar,^{a)} Christopher E. Patrick,^{b)} Rachel S. Edwards,^{b)} Geetha Balakrishnan,^{b)} Martin R. Lees,^{b)} and Julie B. Staunton

AFFILIATIONS

Department of Physics, University of Warwick, Coventry CV4 7AL, United Kingdom

^{a)}Electronic mail: santosh.kumar595@gmail.com

^{b)}Author to whom correspondence should be addressed: m.r.lees@warwick.ac.uk

ABSTRACT

We present pressure-dependent magnetization measurements carried out in the domain of the spin reorientation transitions (SRTs) of a NdCo₅ single crystal. The application of a hydrostatic pressure leads to a shift in the SRTs to higher temperatures. This shift is found to be very sensitive to pressure, with the SRT temperatures increasing at a rate of ≈ 17 K/GPa. To explain the experimental results, we have also performed first-principles calculations of the SRT temperatures for different applied strains, which corroborate the experimental findings. The calculations attribute the pressure dependence of the SRTs to a faster weakening of the Co contribution to the magnetocrystalline anisotropy with pressure compared to the Nd contribution.

Published under license by AIP Publishing. <https://doi.org/10.1063/1.5135640>

The class of intermetallic compounds with the formula RCo₅ (R = rare earth) are archetypal rare-earth transition-metal permanent magnets, displaying high Curie temperatures, large saturation magnetizations, and strong magnetic anisotropy,¹ and have been the subject of intensive investigations both experimentally and theoretically for several decades.^{2–8} RCo₅ crystallizes in the hexagonal *P6₃/mmm* structure with RCo₂ planes interspersed with Co planes.⁹ Magnetically, RCo₅ is a ferrimagnet whose properties derive from two magnetic sublattices associated with rare earth and cobalt atoms. Competition between these sublattices can lead to unusual magnetic behavior, especially as a function of temperature. For example, in GdCo₅, the Gd sublattice, whose moments are aligned antiparallel to the Co moments through an antiferromagnetic exchange interaction, disorders more quickly with temperature than the Co sublattice, and so the magnetization increases with temperature, reaching a peak around 800 K.^{7,10} This faster disordering of the R sublattice is observed across the RCo₅ series because of the weaker exchange interactions for R-Co than Co-Co.¹¹ The antiferromagnetic exchange originates from a strong hybridization of the minority Co-3d and the R-5d bands. The majority Co-3d band, with lower energy, is unable to undergo this hybridization.¹²

The competition between the R and Co sublattices also causes the magnetocrystalline anisotropy (MCA) to behave unusually. The MCA associated with the itinerant electrons forming the Co sublattice favors magnetization parallel to the crystallographic *c*-axis for all members of

the RCo₅ family.¹³ However, the MCA of the R moments originates from the *R-4f* electrons interacting with the crystal field, and whether this interaction favors the *c*-axis or *ab*-plane magnetization depends on R.¹⁴ Among the lighter rare earth elements, R does not contribute to the MCA for Y and La and reinforces the *c*-axis anisotropy for Ce and Sm. Only in PrCo₅ and NdCo₅ does the R contribution to the MCA favor *ab* plane magnetization, competing with the uniaxial anisotropy of the Co moments.⁴ For PrCo₅, the Pr contribution to the MCA is relatively weak, and so at cryogenic temperatures, the magnetization points 23° from the *c*-axis and aligns along *c* at temperatures above 105 K.⁶ However, in NdCo₅, the MCA associated with Nd is strong enough to overcome the Co anisotropy, and so the resultant magnetization lies in the *ab* plane at low temperature.^{6,15}

As the temperature of NdCo₅ is raised, a faster disordering of the R sublattice weakens the Nd planar MCA compared to the uniaxial Co contribution. At a critical temperature *T*_{SR1}, the magnetization starts to rotate toward the *c*-axis (cone anisotropy). This rotation completes at *T*_{SR2}, when the magnetization points along the *c*-axis. The transitions from planar → cone and cone → *c*-axis alignment are referred to as spin reorientation transitions (SRTs).¹⁶ The SRTs of NdCo₅ have been the subject of a number of studies^{3,15–19} and are considered particularly interesting because *T*_{SR1} and *T*_{SR2} are not far from room temperature, at approximately 240 and 290 K, respectively. This work includes our study of NdCo₅ using torque magnetometry, investigating the underlying

physics and location of the SRTs.¹⁵ Interest in NdCo₅ was increased further by the discovery of a giant rotating magnetocaloric effect in NdCo₅ with a maximum adiabatic temperature change observed at 280 K, close to T_{SR2} , suggesting that this material could be used in magnetic refrigeration.²⁰ This observation inspired attempts to bring the operating temperature of the magnetocaloric cycle closer to room temperature, by manipulating T_{SR2} .^{21,22}

Any changes in the *R* or Co MCA will affect the SRT temperatures. Crucially, however, since the SRT temperatures are determined by the balance between sublattices, it is the *relative* MCA enhancement that determines how the SRT temperatures change. Strengthening the *R* contribution relative to Co will favor planar alignment over a wider temperature range increasing T_{SR1} and T_{SR2} . Conversely, strengthening the Co uniaxial anisotropy relative to *R* will decrease T_{SR1} and T_{SR2} .

To date, attempts to change T_{SR2} of NdCo₅ have focused on introducing dopant atoms.^{21–25} For instance, substituting Co with B to form NdCo₄B increases the relative strength of the planar contribution to the extent that planar anisotropy dominates all the way to the Curie temperature so that no SRT is observed.²⁵ Substitution with Al or Si to form NdCo₄Al²¹ or NdCo₄Si²² also shifts the balance in favor of planar anisotropy, but to a lesser extent than in NdCo₄B. Accordingly, these compounds still exhibit SRTs and at elevated temperatures compared to NdCo₅. However, the precise mechanism by which dopant atoms affect the SRTs is not easy to identify. Apart from modifying the electronic band structure, which will alter the Co anisotropy, the introduction of dopants will possibly change the crystal field at the *R* site through both local interactions and also a global modification of the lattice parameters.

In this Letter, we demonstrate an alternative method to manipulate the SRTs by placing NdCo₅ under hydrostatic pressure. Pressure is a “clean” variable that can bring about large changes in the structure and properties without altering the chemical composition. This makes high-pressure states amenable to the computational study. We show that applying pressure shifts the SRT temperatures upward, at a rate of ~ 17 K/GPa. We complement the experimental measurements with finite temperature density-functional theory (DFT) calculations, which also find that the SRT temperatures increase with pressure, at a rate of 12 K/GPa. The calculations show how both the Nd and Co sublattice anisotropies are reduced as a result of applying pressure, but that relatively the decrease is stronger for Co, increasing the SRT temperatures.

The measurements were performed on a single crystal of NdCo₅ grown using the optical floating zone technique.²⁶ This compound has previously been prepared in different forms using other techniques.^{27,28} A crystal of NdCo₅ with a volume of ~ 0.05 mm³ was taken from the same batch used for our recent torque magnetometry study.¹⁵ The crystal was loaded into a cylindrical polytetrafluoroethylene sample holder filled with a pressure transmitting medium (Daphne oil) and placed in an easyLab Mcell 10 beryllium-copper piston clamp pressure cell. Care was taken to ensure that the sample would not move in a magnetic field. Hydrostatic pressure was applied at room temperature. The pressure in the cell was determined *in situ* from the superconducting transition temperature in a magnetic field of 1 mT of a small piece of high purity (99.9999%) tin placed alongside the sample.²⁹ Measurements were carried out between 5 and 320 K. The pressure set at room temperature varies by less than 10% over this temperature range.³⁰ Magnetization measurements as a function of temperature were carried out using a Quantum Design Magnetic Property Measurement System magnetometer.

The strain- and temperature-dependent MCA of NdCo₅ was calculated using the theory introduced in Ref. 31. The *R*-4*f* electrons were treated within single-ion crystal field (CF) theory, where the CF coefficients were calculated from first principles using DFT.³² The Co moments were treated within the disordered local moment formulation of DFT (DFT-DLM),³³ which takes into account the reduction of magnetic order as the temperature is increased. DFT-DLM calculations were also used to parameterize the exchange field entering the CF Hamiltonian, using the scheme introduced in Ref. 8. The same computational setup was used as in previous works,^{31,32} using the GPAW and Hutsepot codes.^{34,35} The easy direction of magnetization was calculated as a function of temperature and lattice parameters, where the experimental values of $a_0 = 5.0055$ Å and $c_0 = 3.9775$ Å as reported in Ref. 36 were used to define the zero-strain structure. Uniform compressive strains of 0.5, 1.0, and 2.0% were applied, where, for instance, a 1% compressive strain corresponds to lattice parameters $a = 0.99a_0$, $c = 0.99c_0$.

Figure 1(a) displays the temperature dependence of the magnetization, $M(T)$, for a NdCo₅ crystal at various pressures. These data were collected while warming the sample at a rate of 1 K/min in an applied field, $\mu_0 H = 0.05$ T. The SRT appears as a broad hump identifiable in all the $M(T)$ curves. The SRTs clearly shift to progressively higher temperatures as the applied pressure is increased up to 0.8 GPa, which is the maximum attainable with the current setup. In principle,

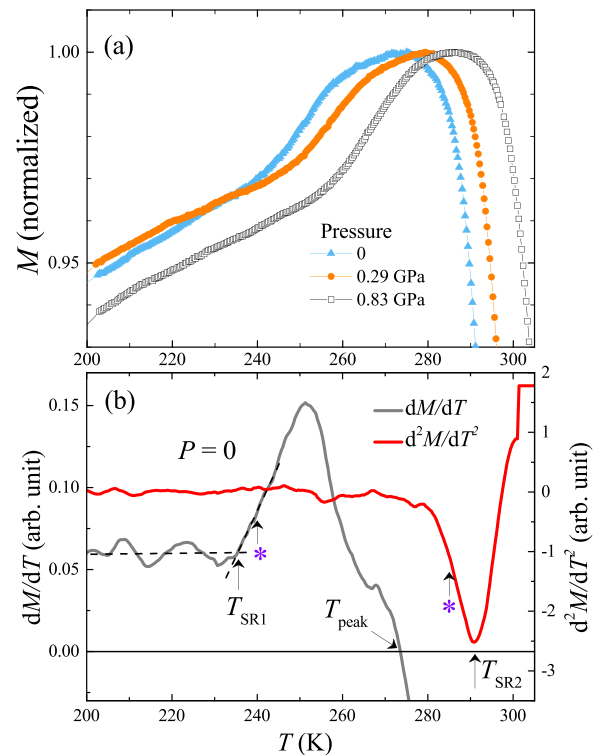


FIG. 1. (a) DC magnetization vs temperature, $M(T)$, for various applied pressures around the SRT region at a field, $\mu_0 H = 0.05$ T. (b) Temperature variation of first and second derivatives of $M(T)$ at ambient pressure. T_{SR1} , T_{peak} , and T_{SR2} have been identified. The asterisks mark the corresponding T_{SR1} (left) and T_{SR2} (right) obtained at $\mu_0 H = 0.5$ T from previous studies.^{15,16}

torque magnetometry provides the clearest identification of temperatures of the SRTs, but unlike DC magnetization measurements, torque magnetometry cannot be performed inside a pressure cell. Instead, to obtain a precise location for T_{SR1} and T_{SR2} , we show in Fig. 1(b) the first and second derivatives of the $M(T)$ curve recorded at ambient pressure. At T_{SR1} (identified by the intersection of the dashed lines), there is a marked increase in dM/dT . This temperature nearly agrees with the T_{SR1} (left asterisk) obtained from our torque measurements¹⁵ as well as from the reported magnetization data.¹⁶ The zero-crossing in dM/dT corresponds to the temperature (T_{peak}) where $M(T)$ is maximum, but there is no clear feature in dM/dT to identify T_{SR2} . However, plotting the second derivative reveals a dip in d^2M/dT^2 that lies just above the T_{SR2} (right asterisk) obtained from our torque study¹⁵ and the reported data.¹⁶ We use these two features—the rise in dM/dT and the minimum in d^2M/dT^2 —as signatures of the SRTs. The two characteristic temperatures (T_{SR1} and T_{SR2}) identified at ambient pressure agree fairly well with our torque study¹⁵ that involved a different protocol of measurements.

DFT-DLM calculations corroborate the experimental measurements. Figure 2 shows the easy direction of magnetization, α , calculated as a function of temperature for different compressive strains, where α is the polar angle with the c -axis. The SRT temperatures bound the region where $0^\circ < \alpha < 90^\circ$. At zero strain, we calculate $T_{\text{SR1}} = 213$ K and $T_{\text{SR2}} = 285$ K; the former is 23 K lower than the experimentally measured value at ambient pressure. Applying 0.5% compressive strain shifts the transition upwards by 35 K. A further increase in the compressive strain increases the SRT temperatures, with T_{SR2} reaching 438 K at 2% strain. We note that the calculated dependence is not linear, which could be a real effect or more likely numerical noise.

Figure 3(a) displays the experimentally measured variation with pressure of T_{SR1} , T_{peak} , and T_{SR2} . For reference, T_{SR1} and T_{SR2} identified from previous studies^{15,16} at ambient pressure are also shown in Fig. 3(a). Both T_{SR1} and T_{SR2} exhibit the same pressure dependence of (17 ± 3) K/GPa. In Fig. 3(b), we show the calculated T_{SR2} values as a function of pressure. Rather than relying on DFT-calculated elastic properties, we use the experimentally measured volume vs pressure

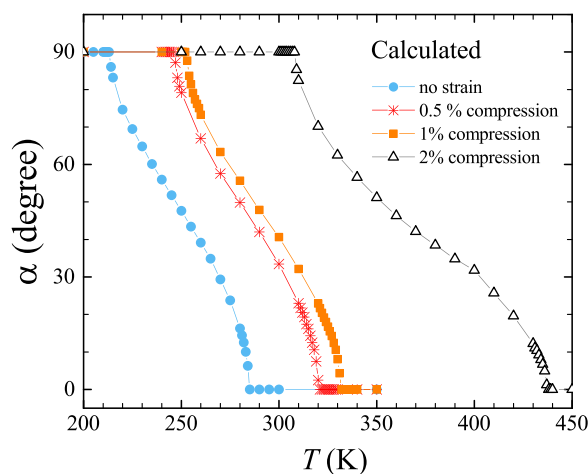


FIG. 2. Temperature variation of the easy angle of magnetization α calculated at different compressive strains.

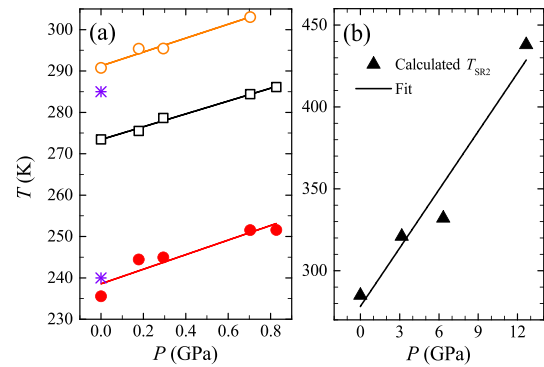


FIG. 3. (a) Pressure dependence of T_{SR1} (●), T_{peak} (□), and T_{SR2} (○) obtained from experiments over the pressure range of $0 \leq P \leq 0.83$ GPa. T_{SR1} and T_{SR2} from our torque magnetometry study¹⁵ at ambient pressure are marked by asterisks. T_{SR2} could not be identified at 0.83 GPa as it has shifted above the upper limit (305 K) of the measured temperature range. (b) Calculated T_{SR2} vs the estimated pressure up to a maximum of 12 GPa.

curve of YCo_5 reported in Ref. 37 to perform an approximate conversion of applied strain into a pressure of 6.3 GPa per 1% strain. Clearly, the strains investigated computationally correspond to significantly larger pressures than those used experimentally, but smaller strains are more prone to numerical noise. A linear fit of the calculated T_{SR2} values gives 12 K/GPa, in reasonable agreement with the experimental value of (17 ± 3) K/GPa.

To explain the increase in the SRT temperatures with pressure, in Fig. 4, we plot the calculated strain dependence of the leading CF

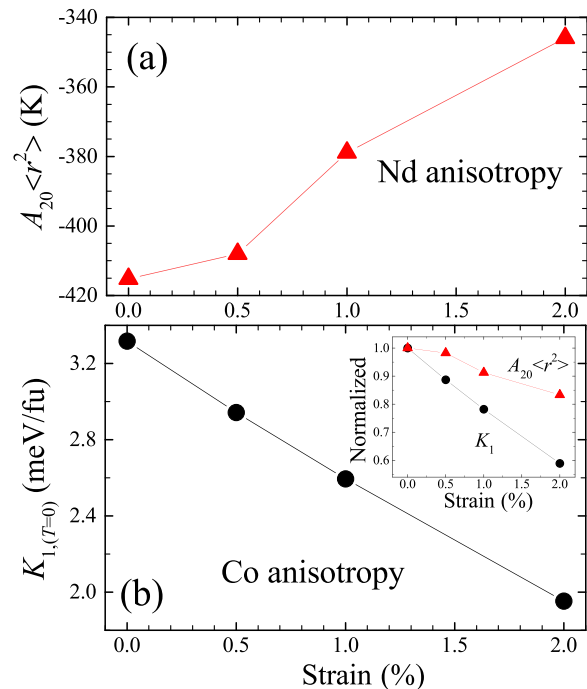


FIG. 4. Pressure dependence of (a) crystal field coefficients, $A_{20}(r^2)$, calculated for the Nd sublattice and (b) the zero temperature anisotropy constants, K_1 of Co.

coefficient $A_{20}\langle r^2 \rangle$ and the zero temperature anisotropy constant associated with the itinerant electrons, K_1 .³¹ These quantities provide the main contribution to the MCA associated with the Nd and Co sublattices, respectively. Both quantities decrease in magnitude as a compressive strain is applied, showing that the MCAs of both sublattices decrease with pressure. Indeed, we verified experimentally that K_1 decreases with pressure by performing magnetization measurements on YCo_5 , which, as Y is nonmagnetic, allows K_1 to be isolated. However, the aspect that is crucial to the SRTs is that the relative decrease with pressure is faster for K_1 than $A_{20}\langle r^2 \rangle$. This behavior is shown in the inset of Fig. 4 where the quantities have been normalized to their zero pressure values. For instance, at 2% strain, K_1 has reduced by 42% compared to $A_{20}\langle r^2 \rangle$, which has only reduced by 17%. The increase in relative strength of the Nd MCA with pressure favors planar anisotropy over a wider temperature range, increasing T_{SR1} and T_{SR2} .

In conclusion, both DC magnetization experiments and DFT-DLM-based calculations have found that the SRT temperatures of NdCo_5 increase with pressure. Furthermore, both methods find the rate of increase to be large, at (17 ± 3) K/GPa and 12 K/GPa, respectively. We note that an applied pressure of 1 GPa is sufficient to raise the cone \rightarrow c -axis SRT—which coincides with the optimum temperature for a magnetocaloric cycle²⁰—to room temperature. The calculations explain the pressure dependence of the SRTs, with a faster decrease in the uniaxial magnetocrystalline anisotropy associated with the Co magnetic sublattice compared to the planar Nd contribution with increasing pressure. Our work demonstrates that the application of pressure may be used to modify the temperatures of the SRTs in both NdCo_5 and other members of the RCo_5 series in a controlled way. The observation that the magnetic phase is extremely sensitive to pressure should also motivate further study of NdCo_5 as a potential barocaloric material.³⁸

See the [supplementary material](#) for the details of magnetization measurements performed under pressure on a single crystal of YCo_5 , which show that K_1 in YCo_5 decreases with pressure.

This work is a part of the PRETAMAG project funded by the Engineering and Physical Sciences Research Council, Grant Nos. EP/M028941/1 and EP/M028771/1. M. Ciomaga Hatnean is acknowledged for assistance with single crystal growth. We thank G. A. Marchant for useful discussions.

REFERENCES

- K. Srnat, G. Hoffer, J. Olson, W. Ostertag, and J. J. Becker, *J. Appl. Phys.* **38**, 1001 (1967).
- K. J. H. Buschow and M. Brouha, *J. Appl. Phys.* **47**, 1653 (1976).
- H. P. Klein, A. Menth, and R. S. Perkins, *Physica* **80B**, 153 (1975).
- A. Ermolenko, *IEEE Trans. Magn.* **12**, 992 (1976).
- H. Yoshie, K. Ogino, H. Nagai, A. Tsujimura, and Y. Nakamura, *J. Magn. Mater.* **70**, 303 (1987).
- E. Tatsumoto, T. Okamoto, H. Fujii, and C. Inoue, *J. Phys. Colloq.* **32**, C1 550 (1971).
- C. E. Patrick, S. Kumar, G. Balakrishnan, R. S. Edwards, M. R. Lees, E. Mendive-Tapia, L. Petit, and J. B. Staunton, *Phys. Rev. Mater.* **1**, 024411 (2017).
- C. E. Patrick, S. Kumar, G. Balakrishnan, R. S. Edwards, M. R. Lees, L. Petit, and J. B. Staunton, *Phys. Rev. Lett.* **120**, 097202 (2018).
- J. H. Wernick and S. Geller, *Acta Crystallogr.* **12**, 662 (1959).
- A. S. Yermolenko, *Fiz. Met. Metalloved.* **50**, 741 (1980).
- C. E. Patrick and J. B. Staunton, *Phys. Rev. B* **97**, 224415 (2018).
- M. S. S. Brooks, O. Eriksson, and B. Johansson, *J. Phys.: Condens. Matter* **1**, 5861 (1989).
- Z. Tie-song, J. Han-min, G. Guang-hua, H. Xiu-feng, and C. Hong, *Phys. Rev. B* **43**, 8593 (1991).
- M. D. Kuz'min and A. M. Tishin, "Theory of crystal field effects in 3d-4f intermetallic compounds, in handbook of magnetic materials," in *Handbook of Magnetic Materials*, edited by K. H. J. Buschow (Elsevier B.V., 2008), Vol. 17, Chap. 3, p. 149.
- S. Kumar, C. E. Patrick, R. S. Edwards, G. Balakrishnan, M. R. Lees, and J. B. Staunton, "Torque magnetometry study of the pin reorientation transition and temperature-dependent magnetocrystalline anisotropy in NdCo_5 ," *J. Phys.: Condens. Matter* (to be published).
- M. M. Ohkoshi, H. Kobayashi, T. Katayama, M. Hirano, T. Katayama, and T. Tsushima, *AIP Conf. Proc.* **29**, 616 (1976).
- J. B. Sousa, A. Moreira, J. M. Del Moral, P. Algarabel, and R. Ibarra, *J. Phys.: Condens. Matter* **2**, 3897 (1990).
- M. Seifert, L. Schultz, R. Schäfer, V. Neu, S. Hankemeier, S. Rössler, R. Frömter, and H. P. Oepen, *New J. Phys.* **15**, 013019 (2013).
- H. Bartholin, B. Van Laar, R. Lemaire, and J. Schweizer, *J. Phys. Chem. Solids* **27**, 1287 (1966).
- S. A. Nikitin, K. P. Skokov, Y. S. Koshkid'ko, Y. G. Pastushenkov, and T. I. Ivanova, *Phys. Rev. Lett.* **105**, 137205 (2010).
- Y. Hu, Q. B. Hu, C. C. Wang, Q. Q. Cao, W. L. Gao, D. H. Wang, and Y. W. Du, *Solid State Commun.* **250**, 45 (2017).
- K. Wang, M. Zhang, J. Liu, H. Luo, and J. Sun, *J. Appl. Phys.* **125**, 243901 (2019).
- M. Sagawa, W. Yamagishi, and Z. Henmi, *J. Appl. Phys.* **52**, 2520 (1981).
- S. C. Ma, D. H. Wang, C. L. Zhang, H. C. Xuan, S. D. Li, Z. G. Huang, and Y. W. Du, *J. Alloys Compd.* **499**, 7 (2010).
- H. Ido, W. E. Wallace, T. Suzuki, S. F. Cheng, V. K. Sinha, and S. G. Sankar, *J. Appl. Phys.* **67**, 4635 (1990).
- R. P. Singh, M. Smidman, M. R. Lees, D. McK. Paul, and G. Balakrishnan, *J. Cryst. Growth* **361**, 129 (2012).
- F. Valdés-Bango, F. J. García Alonso, G. Rodríguez-Rodríguez, L. Morán Fernández, A. Anillo, L. Ruiz-Valdepeñas, E. Navarro, J. L. Vicent, M. Vélez, J. I. Martín, and J. M. Alameda, *J. Appl. Phys.* **112**, 083914 (2012).
- A. Hierro-Rodríguez, J. M. Teixeira, M. Vélez, L. M. Alvarez-Prado, J. I. Martín, and J. M. Alameda, *Appl. Phys. Lett.* **105**, 102412 (2014).
- L. D. Jennings and C. A. Swenson, *Phys. Rev. B* **112**, 31 (1958).
- ML04 03e-Mcell 10 Technical Note, Almax-easyLab (2013).
- C. E. Patrick and J. B. Staunton, *Phys. Rev. Mater.* **3**, 101401 (2019).
- C. E. Patrick and J. B. Staunton, *J. Phys.: Condens. Matter* **31**, 305901 (2019).
- B. L. Györfy, A. J. Pindor, J. Staunton, G. M. Stocks, and H. Winter, *J. Phys. F* **15**, 1337 (1985).
- J. Enkovaara, C. Rostgaard, J. J. Mortensen, J. Chen, M. Dulak, L. Ferrighi, J. Gavnholt, C. Glensvad, V. Haikola, H. A. Hansen, H. H. Kristoffersen, M. Kuusma, A. H. Larsen, L. Lehtovaara, M. Ljungberg, O. Lopez-Acevedo, P. G. Moses, J. Ojanen, T. Olsen, V. Petzold, N. A. Romero, J. Stausholm-Møller, M. Strange, G. A. Tritsarlis, M. Vanin, M. Walter, B. Hammer, H. Häkkinen, G. K. H. Madsen, R. M. Nieminen, J. K. Nørskov, M. Puska, T. T. Rantala, J. Schiøtz, K. S. Thygesen, and K. W. Jacobsen, *J. Phys.: Condens. Matter* **22**, 253202 (2010).
- M. Däne, M. Lüders, A. Ernst, D. Ködderitzsch, W. M. Temmerman, Z. Szotek, and W. Hergert, *J. Phys.: Condens. Matter* **21**, 045604 (2009).
- A. V. Andreev, "Thermal expansion anomalies and spontaneous magnetostriction in rare-earth intermetallics with cobalt and iron," in *Handbook of Magnetic Materials*, edited by K. H. J. Buschow (Elsevier, North-Holland, New York, 1995), Vol. 8, Chap. 2, p. 59.
- D. Koudela, U. Schwarz, H. Rosner, U. Burkhardt, A. Handstein, M. Hanfland, M. D. Kuz'min, I. Opahle, K. Koepfner, K.-H. Müller, and M. Richter, *Phys. Rev. B* **77**, 024411 (2008).
- M. V. Gorev, E. V. Bogdanov, and I. N. Flerov, *J. Phys. D: Appl. Phys.* **50**, 384002 (2017).